Membrane Proteins

Deutsche Ausgabe: DOI: 10.1002/ange.201507332
Internationale Ausgabe: DOI: 10.1002/anie.201507332

A Self-Assembled Respiratory Chain that Catalyzes NADH Oxidation by Ubiquinone-10 Cycling between Complex I and the Alternative Oxidase

*Andrew J. Y. Jones, James N. Blaza, Hannah R. Bridges, Benjamin May, Anthony L. Moore, and Judy Hirst**

Abstract: *Complex I is a crucial respiratory enzyme that conserves the energy from NADH oxidation by ubiquinone-10 (Q_{10}) in proton transport across a membrane. Studies of its energy transduction mechanism are hindered by the extreme hydrophobicity of Q_{10}, and they have so far relied on native membranes with many components or on hydrophilic Q_{10} analogues that partition into membranes and undergo side reactions. Herein, we present a self-assembled system without these limitations: proteoliposomes containing mammalian complex I, Q_{10}, and a quinol oxidase (the alternative oxidase, AOX) to recycle $Q_{10}H_2$ to Q_{10}. AOX is present in excess, so complex I is completely rate determining and the Q_{10} pool is kept oxidized under steady-state catalysis. The system was used to measure a fully-defined K_M value for Q_{10}. The strategy is suitable for any enzyme with a hydrophobic quinone/quinol substrate, and could be used to characterize hydrophobic inhibitors with potential applications as pharmaceuticals, pesticides, or fungicides.*

Mitochondrial complex I (NADH:ubiquinone oxidoreductase) is a crucial energy-transducing respiratory enzyme. It catalyzes NADH oxidation in the matrix and ubiquinone-10 (Q_{10}) reduction in the inner membrane by a process coupled to energy-conserving proton transfer across the membrane.[1] The mechanism of NADH oxidation by the flavin-containing active site has been characterized in detail by using soluble electron acceptors. The mechanism of Q_{10} reduction, an integral part of the unknown coupling mechanism, presents a much greater challenge owing to the extreme hydrophobicity of Q_{10}. Previous studies have addressed the effects of inhibitors[2] and mutations in and around the substrate binding site,[3,4] and made use of spectroscopy to search for ubiqsemiquinone intermediates.[5] However, they have relied on either Q_{10} in native membranes[5,6] (which contain many different enzymes, thus complicating spectroscopic and kinetic analyses) or on non-physiological hydrophilic Q_{10} analogues such as ubiquinone-1, ubiquinone-2 and decylubiquinone (DQ)[4,7] (which must be added in excessive concentrations to maintain steady-state catalysis and that react adventitiously at the flavin to generate damaging reactive oxygen and semiquinone species[8]).

Proteoliposomes (PLs) are artificial phospholipid vesicles into which membrane proteins are reconstituted to mimic their natural environment. PLs suitable for kinetic and spectroscopic studies of Q_{10} reduction by complex I require Q_{10} in the membrane and co-reconstitution of an enzyme to reoxidize $Q_{10}H_2$ (ubiquinol-10, reduced Q_{10}). The alternative oxidase (AOX) is a single-subunit quinol oxidase that catalyzes $Q_{10}H_2$ oxidation and O_2 reduction (but not proton transfer across the membrane).[9] Herein, we present a new, self-assembled respiratory membrane system (termed Q_{10}PLs) that contains mammalian complex I (from *Bos taurus*), Q_{10} (its physiological substrate), and AOX (from *Trypanosoma brucei brucei*; see Scheme 1).

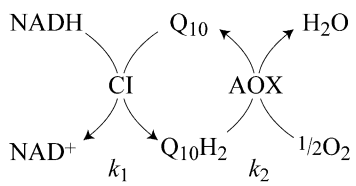

Scheme 1. Q_{10} cycling in the Q_{10}PL membrane. Complex I (CI) oxidizes NADH in the external solution and reduces Q_{10} to $Q_{10}H_2$ in the membrane; AOX reoxidizes the $Q_{10}H_2$ and reduces O_2 to H_2O. k_1 and k_2 are the rate constants for catalysis by complex I and AOX, respectively.

Table 1 presents the catalytic properties of Q_{10}PLs formed with a CI/Q_{10}/AOX molar ratio of 1:800:26 (equal masses of complex I and AOX; see the Supporting Information for experimental details). The highest reported turnover numbers for AOX and *B. taurus* complex I are approximately 500 and 330 s^{-1}, respectively[10,11] (assuming complex I comprises ca. 10% of the protein in mitochondrial membranes[12]). The high CI/AOX ratio is intended to ensure that, during steady-state catalysis, complex I is rate determining and the Q_{10} pool is oxidized. First, to confirm that complex I is rate determining,

[*] A. J. Y. Jones, J. N. Blaza, H. R. Bridges, J. Hirst
Medical Research Council Mitochondrial Biology Unit
Wellcome Trust/MRC Building
Hills Road, Cambridge, CB2 0XY (UK)
E-mail: jh@mrc-mbu.cam.ac.uk

B. May, A. L. Moore
School of Life Sciences, University of Sussex
Falmer, Brighton BN1 9QG (UK)

Supporting information and ORCID(s) from the author(s) for this article are available on the WWW under http://dx.doi.org/10.1002/anie.201507332.

Table 1: Characterization of a typical Q_{10}PL preparation.

Reaction	Specific activity[d] [μmol min^{-1}/mg CI]	Complex I turnover[d] [s^{-1}]	Value determined[d]
1) NADH:O_2	18.6 ± 0.51	309 ± 9	–
2) NADH:O_2 + gramicidin[a]	20.4 ± 0.76	340 ± 13	RCR 1.10 ± 0.05
3) NADH:O_2 + alamethicin[b]	24.6 ± 1.26	410 ± 21	% Oriented 83.0 ± 4.3
4) NADH:DQ + ala[b] + asco[c]	7.64 ± 0.73	127 ± 12	Relative activity vs. (3) 31 ± 3 %
5) NADH:DQ + alamethicin[b]	12.90 ± 0.23	215 ± 4	Relative activity vs. (3) 54 ± 3 %

[a] Gramicidin is an ionophore that dissipates Δp. [b] Alamethicin is a pore-forming antibiotic[13] that allows NADH access to the Q_{10}PL lumen. [c] Ascofuranone is an AOX inhibitor.[14] [d] Mean ± S.E.M. ($n=3$).

Q_{10}PLs were prepared with half the usual amount of complex I (Table S1 in the Supporting Information), and the rate of catalysis was exactly halved. Second, Equation 1 (derived from Scheme 1) indicates that for a 1:26 ratio of complex I and AOX with equal rate constants, the Q_{10} pool is 96 % oxidized. Finally, complex I in Q_{10}PLs catalyzes at up to 400 s^{-1} (see Table 1), which is faster than in native membranes (in which $Q_{10}H_2$ reoxidation is rate limiting).

$$\frac{[Q_{10}]}{[Q_{10}]+[Q_{10}H_2]} = \frac{[AOX]k_2}{[CI]k_1 + [AOX]k_2} \quad (1)$$

Q_{10}PLs allow direct comparison of complex I catalysis using Q_{10} with catalysis using its hydrophilic analogue DQ.[7] Catalysis with 100 μM DQ (molar CI/DQ ratio 1:200,000) was measured with Q_{10}-free CI/AOX PLs, with AOX inhibited by ascofuranone[14] to prevent DQH_2 reoxidation. Complex I turnover was three times slower than with Q_{10} (127 vs. 410 s^{-1}, see Table 1). However, the rate increased to 215 s^{-1} when AOX was allowed to oxidize DQH_2 in the membrane, which matches the rate of NADH:DQ oxidoreduction by the detergent-solubilized complex I used to prepare the (Q_{10})PLs (233 ± 53 s^{-1}), and also the rate from (Q_{10})PLs resolubilized by detergent addition. Therefore, steady-state reduction of DQ by complex I in (Q_{10})PLs is hindered by accumulation of DQH_2 in the membrane and its slow exchange for DQ across the membrane interface. Our results highlight three important advantages of a reconstituted Q_{10} system for studying the quinone chemistry of complex I: the rapid kinetics of Q_{10} reduction, the physiological relevance of Q_{10}, and the simplicity of having all of the Q_{10} species confined to the membrane with no exchange across the membrane interface.

There are two well-established methods for assessing proton-motive force (Δp) formation by respiratory enzymes in PLs, a central requirement for mechanistic studies. First, substantial quenching of the fluorescence of 9-amino-6-chloro-2-methoxyacridine (ACMA) during NADH oxidation by Q_{10}PLs indicates the formation of a substantial ΔpH (Figure 1 A).[15] Second, the respiratory control ratio (RCR) is

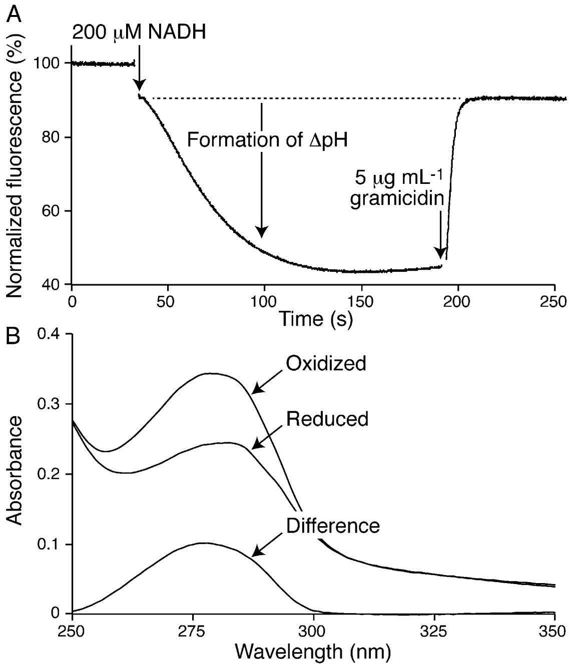

Figure 1. Analyses of ΔpH formation and Q_{10} concentration in Q_{10}PLs. A) Formation of ΔpH across the PL membrane is demonstrated by quenching of ACMA fluorescence. Gramicidin collapses Δp and the fluorescence returns to its starting value. Conditions: 4 μg mL^{-1} complex I and 6 μg mL^{-1} AOX in Q_{10}PLs containing ca. 20 nmol Q_{10}/mg phospholipid in 10 mM Tris-SO_4 (pH 7.5), 50 mM KCl, 75 mM KNO_3, and 0.5 μM ACMA, 32 °C. B) Spectroscopic determination of Q_{10} concentration in a Q_{10}PL preparation. The spectra are from Q_{10}PLs that have been solubilized with 1 % sodium dodecyl sulfate (SDS) before (oxidized) and after (reduced) addition of 1.5 mM KBH_4 to reduce the Q_{10} to $Q_{10}H_2$. The intensity of the difference spectrum at 275 nm denotes the Q_{10} concentration. Concentrations present: 11.8 nM complex I, 0.6 μM AOX, 0.472 mg mL^{-1} phospholipid, and 6.88 μM Q_{10} (calculated).

the ratio of the coupled and uncoupled rates of catalysis: Δp opposes catalysis, so when an "uncoupler" is used to dissipate Δp, the rate increases. The RCR value for NADH oxidation by Q_{10}PLs (1.1, 4 H^+ translocated per NADH) is low compared to values reported for submitochondrial particles (3.0–5.5,[11,12,16] 10 H^+ per NADH for complexes I, III, and IV) and complex I containing PLs measured using DQ (2.2–4.5,[17,18] 4 H^+ per NADH) However, lower values are typical for succinate oxidation by SMPs (1.6–3.2,[11,12,16] 6 H^+ per succinate from complexes II, III and IV), and the highest value from inverted *Escherichia coli* vesicles that are known to sustain $\Delta p \approx 160$ mV[19] is 1.7[20] (6 H^+ per NADH, from complex I and an ubiquinol oxidase). Higher RCR values are usually taken to indicate "better coupled" vesicles, but the values are also affected by the enzyme activity and configuration. More highly active or tightly packed proton-pumping enzymes are better able to compete with proton leak back across the membrane, so they push Δp higher. During steady-state catalysis, proton leak and translocation are equal and opposite: because leak increases with Δp,[21] the more active or packed enzyme reaches a higher Δp but displays a lower

RCR. Therefore, it is not currently possible to quantify the Δp sustained by complex I in Q_{10}PLs. The pore-forming antibiotic alamethicin[13] was used in all subsequent experiments to dissipate Δp and prevent it from confounding the results.

Q_{10}PLs are a unique respiratory system because all of their components are known and can be quantified (see the Supporting Information). Complex I concentrations were quantified using the flavin-catalyzed NADH:APAD$^+$ oxidoreduction reaction,[22] and AOX concentrations were taken to be the difference between the total protein and complex I concentrations. Phospholipid concentrations were quantified by phosphate determination[23] and Q_{10} concentrations were determined spectroscopically by measuring the absorbance change upon addition of KBH_4 (a reducing agent, see Figure 1B).[24] Table S1 shows the values from a set of Q_{10}PLs containing different Q_{10} concentrations. Finally, density-gradient centrifugation was used to check the homogeneity of a high-Q_{10} preparation of Q_{10}PLs. Two distinct bands were observed: the denser band contained approximately 80% of the phospholipid and roughly 90% of the complex I. The vesicles in the less dense band may contain less complex I because they became less saturated with detergent during reconstitution. Crucially, both bands contained the same phospholipid/Q_{10} ratio, so the minor inhomogeneity present was not considered significant.

Figure 2 shows the rate of NADH:O_2 oxidoreduction by complex I in Q_{10}PLs as a function of Q_{10} concentration, defined using the phospholipid concentration as a proxy for the hydrophobic/membrane phase volume. The complex I/Q_{10} ratio is fixed in the preparation, so standard solution kinetic analyses are not possible and each point is from an independent preparation. The fact that the preparation with half the usual complex I content has a matching rate of turnover confirms that the rate is set only by the Q_{10} concentration (complex I is diluted in the membrane but the Q_{10} concentration is constant). The data in Figure 2 were fit to the Michaelis–Menten equation, giving a K_M (Q_{10}) value for *B. taurus* complex I of 3.9 nmol/mg phospholipid (approximately one Q_{10} molecule per 300 phospholipids). To our knowledge this is the first steady-state K_M measurement for an enzyme and its native quinone, for which the quinone substrate pool is held fully oxidized in every condition tested. Previously, elegant single-turnover kinetics on *Rhodobacter* complex III in chromatophores defined $K_M(Q_{10}H_2) = 3–5$ $Q_{10}H_2$ per complex, but using a "collisional mechanism" in which the rate is determined by $[Q_{10}H_2]$ and unaffected by $[Q_{10}]$.[26] For complex I, a value of $K_M(Q_{10}) = 2.4 \pm 1.7$ nmol/mg protein (consistent with our value) was reported using pentane-extracted mitochondria (but with the redox state of the Q pool undefined).[27]

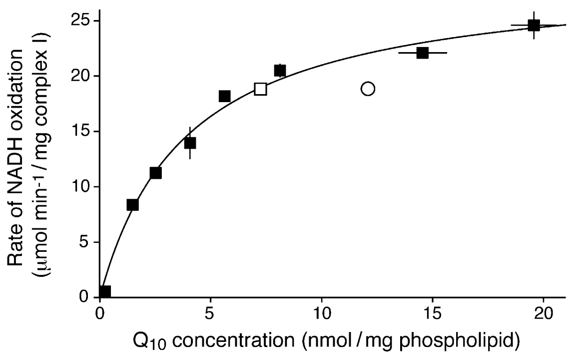

Figure 2. Q_{10} Michaelis–Menten curve for *B. taurus* complex I. The rates of NADH oxidation from different Q_{10}PL preparations are plotted against the Q_{10} concentrations in the membranes and fit to the Michalis–Menten equation with $K_M = 3.94$ nmol/mg phospholipid and $k_{cat} = 29.9$ μmol min^{-1}/mg complex I = 500 s^{-1}. Open square: Q_{10}PL preparation with half the standard amount of complex I. Open circle: complex I in *B. taurus* mitochondrial membranes (rate of catalysis enhanced by additional cytochrome *c*[25]). Conditions: 200 μM NADH, 15 μg mL^{-1} alamethicin (Q_{10}PLs only), 10 mM Tris-SO_4 (pH 7.5), and 50 mM KCl, 32 °C. Values are the mean ± S.E.M. ($n = 3$).

Figure 2 also shows our value for complex I turnover in *B. taurus* heart mitochondrial membranes that contain approximately 12 nmol Q_{10}/mg phospholipid (ca. 60 Q_{10} per complex I; see Table S2). Because the membrane Q_{10} concentration is three times the complex I K_M value, respiratory-chain turnover in membranes is not limited at complex I by Q_{10} pool concentration. The membrane data point in Figure 2 falls below the curve owing to rate-limiting contributions from complexes III and IV (which also render the Q_{10} pool partially reduced).

The K_M (Q_{10}) value of 3.9 nmol Q_{10}/mg phospholipid equates to approximately 3.9 mM Q_{10} in the membrane phase because 1 mg of phospholipid has a volume of around 1 μL.[28] The value is high in comparison to values for enzymes that act on soluble substrates, but Q_{10} is restricted to diffusion only within the two-dimensional membrane bilayer, and the K_M tells us little about K_D (only that $K_D \leq 3.9$ mM). With such a high local Q_{10} concentration, there is no pressure on complex I to evolve a lower K_M, and matching K_M to concentration may help the system respond to changing conditions. Furthermore, the high concentration creates sufficient capacity to buffer changes to the Q_{10} pool potential, and may facilitate antioxidant reactions that rely on the (uncatalyzed) second-order reactions of Q_{10} and $Q_{10}H_2$ with radical species.[29]

Q_{10}PLs are independent respiratory units formed by self-assembly from a mixture of phospholipids, Q_{10}, complex I, and AOX. Complex I (from *B. taurus* heart) and AOX (from *T. brucei*) originate from very different sources and assemble independently into Q_{10}PLs, thus making non-physiological supercomplex assemblies highly unlikely and imposing the fluid mosaic model[30] on the membrane. The rapid rates of catalysis observed support the interpretation that supercomplexes are not necessary for efficient catalysis and argue further against a role for Q_{10} channeling within them.[25]

Self-assembled artificial respiratory chains are suitable for biophysical studies of any respiratory or photosynthetic enzyme that uses a membrane-bound quinone substrate. Historically, they were used to demonstrate the construction of respiratory chains from individual enzymes and Q_{10}, but their capabilities have not (with very few exceptions[31]) been exploited for detailed mechanistic studies. Furthermore, many quinone antagonists are already used as pharmaceuticals or pesticides,[32,33] and bioenergetic enzymes specific to parasites and phytopathogenic fungi (including the alternative NADH dehydrogenase and AOX) are being investigated as drug targets.[34,35] Our self-assembled Q_{10}PL system enables candidate drugs and inhibitors to be competed against physiologically relevant quinone substrates to provide properly defined and robust inhibitor dissociation constants for translational research.

Acknowledgements

This research was funded by The Medical Research Council (grant U105663141 to J.H.), BBSRC (BB/L022915/1 to A.L.M.) and the University of Sussex.

Keywords: electron transport chain · NADH · oxidoreductases · proteoliposomes · quinones

How to cite: *Angew. Chem. Int. Ed.* **2016**, *55*, 728–731
Angew. Chem. **2016**, *128*, 738–741

[1] J. Hirst, *Annu. Rev. Biochem.* **2013**, *82*, 551–575.
[2] T. Ito, M. Murai, H. Morisaka, H. Miyoshi, *Biochemistry* **2015**, *54*, 3677–3686.
[3] P. K. Sinha, N. Castro-Guerrero, G. Patki, M. Sato, J. Torres-Bacete, S. Sinha, H. Miyoshi, A. Matsuno-Yagi, T. Yagi, *Biochemistry* **2015**, *54*, 753–764.
[4] M. A. Tocilescu, U. Fendel, K. Zwicker, S. Kerscher, U. Brandt, *J. Biol. Chem.* **2007**, *282*, 29514–29520.
[5] A. D. Vinogradov, V. D. Sled, D. S. Burbaev, V. G. Grivennikova, I. A. Moroz, T. Ohnishi, *FEBS Lett.* **1995**, *370*, 83–87.
[6] A. Kröger, M. Klingenberg, *Eur. J. Biochem.* **1973**, *34*, 358–368.
[7] E. Estornell, R. Fato, F. Pallotti, G. Lenaz, *FEBS Lett.* **1993**, *332*, 127–131.
[8] M. S. King, M. S. Sharpley, J. Hirst, *Biochemistry* **2009**, *48*, 2053–2062.
[9] T. Shiba, Y. Kido, K. Sakamoto, D. K. Inaoka, C. Tsuge, R. Tatsumi, G. Takahashi, E. O. Balogun, T. Nara, T. Aoki, et al., *Proc. Natl. Acad. Sci. USA* **2013**, *110*, 4580–4585.
[10] Y. Kido, K. Sakamoto, K. Nakamura, M. Harada, T. Suzuki, Y. Yabu, H. Saimoto, F. Yamakura, D. Ohmori, A. Moore, et al., *Biochim. Biophys. Acta* **2010**, *1797*, 443–450.
[11] A. D. Vinogradov, V. G. Grivennikova, *Biochemistry* **2005**, *70*, 120–127.
[12] K. R. Pryde, J. Hirst, *J. Biol. Chem.* **2011**, *286*, 18056–18065.
[13] I. S. Gostimskaya, V. G. Grivennikova, T. V. Zharova, L. E. Bakeeva, A. D. Vinogradov, *Anal. Biochem.* **2003**, *313*, 46–52.
[14] C. Nihei, Y. Fukai, K. Kawai, A. Osanai, Y. Yabu, T. Suzuki, N. Ohta, N. Minagawa, K. Nagai, K. Kita, *FEBS Lett.* **2003**, *538*, 35–40.
[15] S. Grzesiek, H. Otto, N. A. Dencher, *Biophys. J.* **1989**, *55*, 1101–1109.
[16] A. B. Kotlyar, A. D. Vinogradov, *Biochim. Biophys. Acta Bioenerg.* **1990**, *1019*, 151–158.
[17] A. Galkin, S. Dröse, U. Brandt, *Biochim. Biophys. Acta Bioenerg.* **2006**, *1757*, 1575–1581.
[18] P. G. Roberts, J. Hirst, *J. Biol. Chem.* **2012**, *287*, 34743–34751.
[19] W. W. Reenstra, L. Patel, H. Rottenberg, H. R. Kaback, *Biochemistry* **1980**, *19*, 1–9.
[20] C. Burstein, L. Tiankova, A. Kepes, *Eur. J. Biochem.* **1979**, *94*, 387–392.
[21] D. G. Nicholls, *Eur. J. Biochem.* **1974**, *50*, 305–315.
[22] G. Yakovlev, J. Hirst, *Biochemistry* **2007**, *46*, 14250–14258.
[23] B. N. Ames, *Methods Enzymol.* **1966**, *8*, 115–118.
[24] R. Covian, B. L. Trumpower, *J. Biol. Chem.* **2005**, *280*, 22732–22740.
[25] J. N. Blaza, R. Serreli, A. J. Y. Jones, K. Mohammed, J. Hirst, *Proc. Natl. Acad. Sci. USA* **2014**, *111*, 15735–15740.
[26] G. Venturoli, J. G. Fernández-Velasco, A. R. Crofts, B. A. Melandri, *Biochem. Biophys. Acta* **1986**, *851*, 340–352.
[27] E. Estornell, R. Fato, C. Castelluccio, M. Cavazzoni, G. Parenti Casteli, G. Lenaz, *FEBS Lett.* **1992**, *311*, 107–109.
[28] G. C. Newman, C. Huang, *Biochemistry* **1975**, *14*, 3363–3370.
[29] A. M. James, R. A. J. Smith, M. P. Murphy, *Arch. Biochem. Biophys.* **2004**, *423*, 47–56.
[30] S. J. Singer, G. L. Nicolson, *Science* **1972**, *175*, 720–731.
[31] G. Venturoli, N. Gabellini, D. Oesterhelt, B. A. Melandri, *Eur. J. Biochem.* **1990**, *189*, 95–103.
[32] P. R. Rich, *Pestic. Sci.* **1996**, *47*, 287–296.
[33] K. B. Wallace, A. A. Starkov, *Annu. Rev. Pharmacol. Toxicol.* **2000**, *40*, 353–388.
[34] E. A. Weinstein, T. Yano, L. S. Li, D. Avarbock, A. Avarbock, D. Helm, A. A. McColm, K. Duncan, J. T. Lonsdale, H. Rubin, *Proc. Natl. Acad. Sci. USA* **2005**, *102*, 4548–4553.
[35] H. Saimoto, Y. Kido, Y. Haga, K. Sakamoto, K. Kita, *J. Biochem.* **2013**, *153*, 267–273.

Received: August 6, 2015
Revised: September 28, 2015
Published online: November 23, 2015

